Seasonal variations of gravity wave activity in the lower stratosphere over an Antarctic Peninsula station

T. Moffat-Griffin,[1] R. E. Hibbins,[1,2] M. J. Jarvis,[1] and S. R. Colwell[1]

Received 18 November 2010; revised 18 May 2011; accepted 31 May 2011; published 26 July 2011.

[1] An 8 year series of 965 high-resolution radiosonde soundings over Rothera (67°S, 68°W) on the Antarctic Peninsula are used to study gravity wave characteristics in the lower stratosphere. The gravity wave energy is shown to have a seasonal variation with peaks at the equinoxes; the largest peak is around the spring equinox. During the winter months and extending into the spring, there is both an enhancement in the downward propagating wave activity and a reduction in the amount of critical-level filtering of upward propagating mountain waves. The horizontal propagation directions of the gravity waves were determined using hodographs. It was found that there is a predisposition toward northward and westward propagating waves above Rothera. This is in agreement with previous observations of gravity wave momentum flux in the wintertime mesosphere over Rothera. These results are consistent with a scenario whereby the stratospheric gravity wavefield above Rothera is determined by a combination of wind flow over topography-generating waves from below, and sources such as the edge of the polar stratospheric vortex-generating waves from above, especially during winter and spring.

Citation: Moffat-Griffin, T., R. E. Hibbins, M. J. Jarvis, and S. R. Colwell (2011), Seasonal variations of gravity wave activity in the lower stratosphere over an Antarctic Peninsula station, *J. Geophys. Res.*, *116*, D14111, doi:10.1029/2010JD015349.

1. Introduction

[2] The dynamics of the middle atmosphere is strongly influenced by gravity waves through wave-mean flow interaction. Gravity waves have short spatial scales and as such cannot be resolved in most of the current global circulation models. To reproduce their effects on the large-scale dynamics of the atmosphere combinations of orographic and nonorographic gravity wave drag parameterizations are implemented in the models. Some models use nonorographic gravity wave parameterizations that assume a fixed gravity wave source spectrum which does not respond to changing weather (e.g., large-scale weather systems), however there has been recent work on including nonorographic gravity wave parameterizations which interact with the climate [*Fritts and Alexander*, 2003; *Kim et al.*, 2003]. In order to properly represent the impact of gravity waves on the atmosphere, both a realistic source spectrum and its variability need to be characterized [*McLandress and Scinocca*, 2005] and this information will come from further detailed gravity wave observational studies and case studies which provide more statistical information on the seasonal and global variability of gravity waves and their sources, propagation and dissipation [e.g., *Alexander et al.*, 2008; *Guharay et al.*, 2010; *Ki and Chun*, 2010; *McDonald et al.*, 2010; *Yan et al.*, 2010; *Zhang et al.*, 2010]. Quantifying these parameters is especially important over Antarctica where gravity waves have been shown to have an influence on ozone depletion via their role in the formation of polar stratospheric clouds (PSCs) [*Cariolle et al.*, 1989; *McDonald et al.*, 2009; *Noel et al.*, 2008]. Studies of satellite data have shown that there can be an enhancement of PSCs over the Antarctic Peninsula [*Hoepfner et al.*, 2006; *McDonald et al.*, 2009], which is a region of intense gravity wave activity. Hence it is especially important to understand wave variability in thus Antarctic Peninsula region.

[3] Observations of gravity waves over Antarctica have been made using a wide range of ground based instruments (e.g., airglow imagers, radiosondes, lidar and radars), superpressure balloons and satellites (e.g., MLS, CHAMP/GPS) [*Alexander et al.*, 2010; *Baumgaertner and McDonald*, 2007; *Espy et al.*, 2006; *Hertzog et al.*, 2008; *Hibbins et al.*, 2007; *Wu and Jiang*, 2002; *Yamashita et al.*, 2009]. These data cover a range of altitudes from the troposphere to the lower thermosphere and also different parts of the gravity wave spectrum (owing to observational filtering) [*Alexander*, 1998]. The gravity wave spectrum covers timescales from a few minutes to several hours and horizontal wavelengths from 100 m to 1000 km. Each measurement technique is biased toward a particular part of the spectrum and has limitations in the range of horizontal and vertical wavelengths that it can resolve. The additional filtering and modification that the waves experience as they propagate makes for additional difficulties in seeing the whole picture from a single set of observations. For instance, satellite observations typically sample waves with

[1] British Antarctic Survey, Cambridge, UK.
[2] Now at Department of Physics, Norwegian University of Science and Technology, Trondheim, Norway.

0148-0227/11/2010JD015349

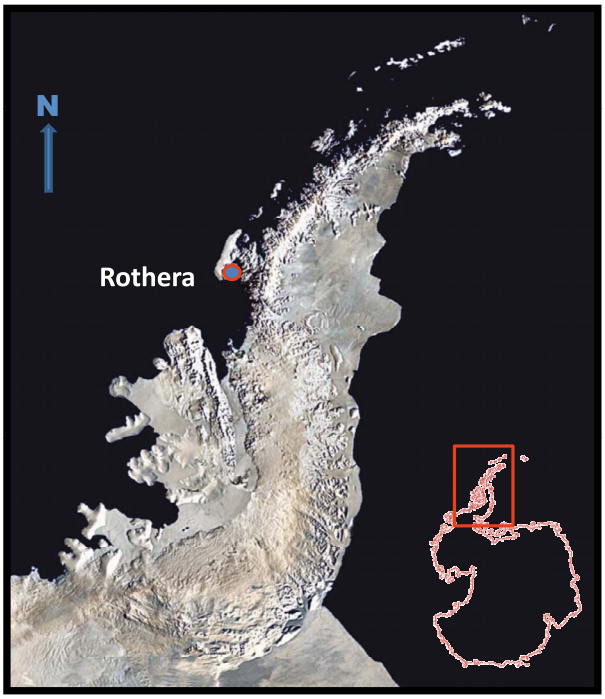

Figure 1. Map showing the Antarctic Peninsula and location of Rothera research station (which is located at 67°S, 68°W).

long vertical wavelengths because they integrate over altitude. This can change dependent upon the viewing geometry of the satellite as demonstrated by *Wu and Jiang* [2002] (remote sounding of atmospheric gravity waves with satellite limb and nadir techniques). Satellite observations from CRISTA [*Ern et al.*, 2004] have shown the Antarctic Peninsula to be a global hot spot for gravity waves in the stratosphere typically with vertical wavelengths of ~17 km and horizontal wavelengths of ~900 km; for CRISTA the measureable vertical wavelength range is ~5 to ~25 km with a lower limit of horizontal wavelength of ~600 km. Using a lidar at Rothera, *Yamashita et al.* [2009] found the gravity wave spectrum between 30 and 45 km altitude to be characterized by vertical wavelengths predominantly less than 6 km; 6 km is the vertical wavelength below which the measurement capability of CRISTA sharply falls off [*Preusse et al.*, 2002]. Conversely, the balloon measurements presented here sample short vertical wavelengths owing to the limited altitude range over which the observations are made. The different data sets therefore complement each other and it can also be seen that care is required when interpreting the data to take into account the limitations of the technique.

[4] Much of the wave energy over the Antarctic Peninsula is generated from the interaction of surface winds with the "knife edge" topography of the Peninsula [*Baumgaertner and McDonald*, 2007; *Hertzog et al.*, 2008; *Plougonven et al.*, 2008]. Several studies [*Nastrom and Fritts*, 1992; *Wu and Jiang*, 2002] have shown that airflow over mountainous regions generates a significant proportion of the overall gravity wave activity and that critical-level filtering can prevent vertical propagation. *Whiteway et al.* [1997] and *Yoshiki et al.* [2004] showed gravity wave enhancements at the edge of the polar vortex in the Northern and Southern Hemispheres, respectively. While Whiteway et al. attributed this to the reduced filtering of orographic waves, Yoshiki et al. attributed it to gravity waves generated at the edge of the vortex.

[5] These observations have shown that the Antarctic Peninsula exhibits among the largest gravity wave amplitudes and energy densities in the world. The Antarctic Peninsula is a narrow 1300 km northward extension of Antarctica toward the southern tip of South America and forms a topographical barrier to the prevailing westerly winds. It is ~900 m altitude at its northern end (~63.5°S), and rises to between ~1750 and ~2000 m between 64°S and 68°S. Further observations of stratospheric gravity waves above the Antarctic Peninsula are therefore required to help understand the relative influences of orography and stratospheric and tropospheric processes on the observed gravity wave variability.

[6] Radiosondes have been used for many gravity wave studies in the troposphere and stratosphere [*Allen and Vincent*, 1995; *Vincent and Alexander*, 2000; *Whiteway et al.*, 1997]. They have the advantage that they can provide vertical profiles of wave activity from the surface to the stratosphere. Radiosondes are also the only instrument that can measure u′, v′ and T′ independently of gravity waves, assuming that the perturbations are caused by the same gravity waves all parameters can be derived from one profile. In the Antarctic, a statistical study of gravity wave activity using radiosonde data [*Yoshiki and Sato*, 2000] showed that there was a peak in gravity wave activity over Antarctica in the spring, and that the likely source of this activity was mainly in the stratosphere. However, their study did not include any data from stations on the mainland Antarctic Peninsula. The purpose of this paper is to investigate the gravity wave characteristics in the lower stratosphere above Rothera using radiosonde data. Rothera, a British Antarctic Survey research station, is ideally located for studies of the Peninsula gravity wave "hotspot." Rothera (68°S), which is situated to the west of the Peninsula on the southeast coast of Adelaide Island (see Figure 1), is ~100 km west of the center of the Peninsula which, at that latitude, is ~70 km wide. Also it is located in the vicinity of the edge of the stratospheric polar vortex where gravity wave activity has been shown to maximize [*Whiteway et al.*, 1997]. Climatologies of the gravity wave energy and propagation directions are derived from 8 years of data, seasonal variations are quantified and likely source regions are investigated.

2. Data

[7] A regular high-resolution radiosonde launch program has been operating at Rothera (67°S, 68°W) for meteorological studies since early 2002. This has consisted of 2 to 4 launches per week, where the launches are timed for 11:00 UT. Up to March 2007, the radiosonde system used at Rothera was a Vaisala RS80, thereafter all radiosondes used were Vaisala RS92. *Steinbrecht et al.* [2008] have compared the performance of RS80 and RS92 radiosondes. There are small systematic differences. On average the RS80 sondes provide much less accurate pressure and geopotential height, and lower temperatures than the RS92 sondes. Temperature differences range from less than 0.1 K below 100 hPa to 0.7 K at 10 hPa. On average the RS80 sondes give up to 1 hPa higher pressure and 20 m lower heights than RS92

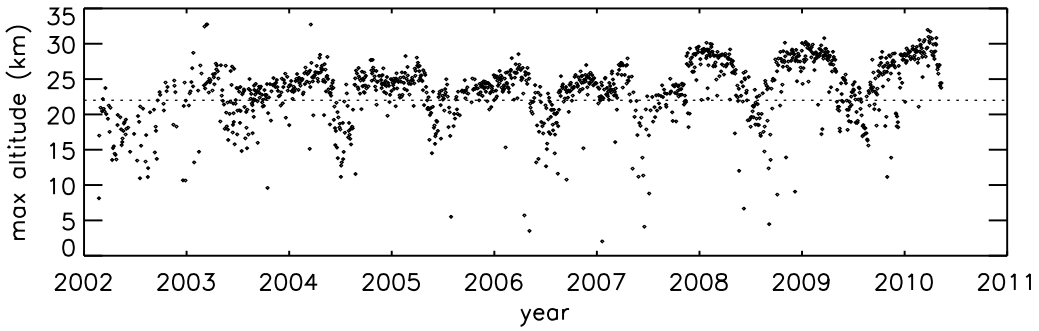

Figure 2. Maximum altitude reached by the radiosonde balloon for every launch at Rothera from 22 February 2002 to 11 May 2010.

sondes in the troposphere, but 0.4 hPa lower pressure and 100 m higher height in the stratosphere. Since the gravity wave detection is derived independently from individual sonde flights and the gravity wave perturbations are relative rather than absolute to the prevailing smoothed altitude profile these small percentage differences between the two sonde types are very unlikely to affect the gravity wave measurements. There is a strong suggestion from visual inspection of Figure 2 that the radiosonde ending height systematically increases after 2007, when the instrument changed from RS80 to RS92. Only a small (~100 m) part of the apparent change of ~3 km in maximum altitude can be attributed to the differences measured by *Steinbrecht et al.* [2008]. Since we are using an upper altitude of at least 22 km as the inclusion criterion for sonde flights in the analysis, this better success rate at higher altitudes for RS92 is unlikely to affect the results. The only difference it might make would be the inclusion of more flights during winter when burst altitudes are low, but no significant decrease in rejected flights in winter is observed after 2007. The data returned are composed of vertical profiles of pressure, temperature, relative humidity, dew point, radiosonde position, wind speed and wind direction. Measurements are taken at either 2 or 10 s intervals and the ascents typically extend to altitudes of ~20–30 km. The wind speed and direction is determined using the GPS signal from the radiosonde. The results presented here are taken from data recorded between 22 February 2002 and 11 May 2010, a total of 1344 balloon launches, although for this paper only 965 complied with the analysis constraints.

[8] Figure 2 shows the maximum altitude reached by the radiosonde balloons for each and every launch. There is a clear seasonal variation in the maximum altitude reached (owing to seasonal changes in atmospheric density) and an increase in this maximum altitude in later years (owing to changes in the preparation of the radiosonde balloon before the launch). For the purposes of this study, the maximum altitude used over the whole data set is 22 km. For height-averaged data analysis this altitude is used as a cutoff point and any balloon thatdoes not reach this altitude is excluded to reduce any seasonal bias in the vertical wavelength spectrum sampled. Of the 1344 launches only 965 meet this criterion. The minimum altitude used for this study is 15 km; this has been chosen to avoid any sharp temperature gradients at the tropopause, which varies between 10 and 13 km altitude over Rothera [*Baumgaertner and McDonald*, 2007]. Sharp temperature gradients affect the calculation of potential energy and the horizontal propagation direction of the gravity waves, both of which require accurate temperature perturbation measurements; therefore these parameters would be inaccurate across the tropopause.

3. Gravity Wave Analysis

3.1. Gravity Wave Energy

[9] Using the wind and temperature perturbation data it is possible to determine the kinetic and potential energy in the stratosphere and troposphere. The first-order perturbations were calculated, following the method of *Vincent and Alexander* [2000] by fitting a second-order polynomial to the wind and temperature profiles over the altitude range and subtracting this fit from the original profile. Figure 3 shows an example of wind speed data from 5 January 2009, the polynomial fit and the resulting wind perturbation. It can be seen that the resulting wind speed profile, determined as the radiosonde rises in altitude, exhibits a wavelike structure which is assumed to be purely due to gravity waves perturbing the prevailing wind. Each profile, spanning 15–22 km altitude, is first interpolated onto a 50 m

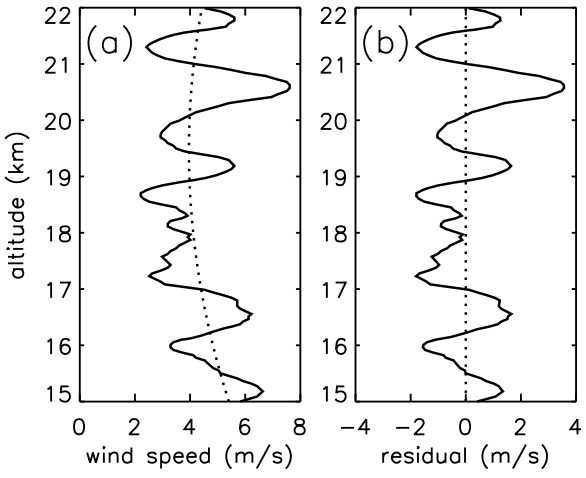

Figure 3. (a) Wind speed (solid line) as measured by the radiosonde on 5 January 2009 between 15 and 22 km fitted with a second-order polynomial (dotted line). (b) Residual wind perturbation when the polynomial is subtracted from the profile.

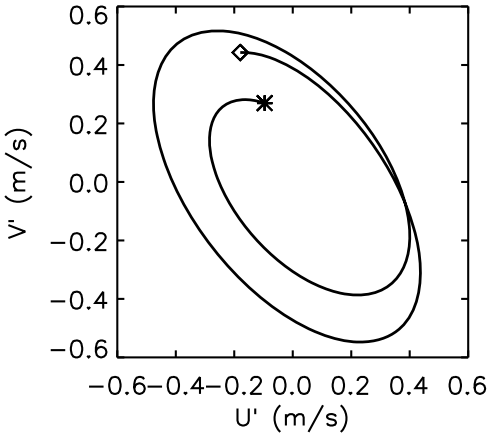

Figure 4. Meridional wind perturbation plotted against the zonal wind perturbation from an individual wave packet measured on 5 January 2009 by a radiosonde. The asterisk indicates the lowest altitude measurements; the diamond indicates the highest altitude measurements.

height grid, then the total gravity wave energy per unit mass is calculated [*Vincent et al.*, 1997] from:

$$E_0 = \frac{1}{2}\left[\overline{u'^2} + \overline{v'^2} + \overline{w'^2} + \frac{g^2\overline{\hat{T}'^2}}{N^2}\right] \quad (1)$$

where $\overline{u'^2}$, $\overline{v'^2}$ and $\overline{w'^2}$ represent the zonal, meridional and vertical components of the wind perturbations (to the first order) squared. $\overline{\hat{T}'^2}$ is the normalized temperature fluctuation, defined as the ratio of the temperature perturbation to the background temperature. The overbar signifies an unweighted average over height. It is assumed that the vertical wind component is small compared to the horizontal components and hence can be ignored [*Vincent et al.*, 1997]. The last term in the equation represents the potential energy per unit mass and the first three terms combined represent the kinetic energy per unit mass.

3.2. Gravity Wave Propagation Direction

[10] Gravity wave parameters, such as propagation direction, that are determined from the vertical profiles of wind and temperature assume the presence of a single monochromatic wave [*Zink and Vincent*, 2001]. This is not always the real case, however, and the presence of multiple waves in the data make the results more difficult to interpret. To ensure that only single waves are studied our analysis uses the wavelet technique outlined in the work of *Zink and Vincent* [2001]. This technique analyses the wind and temperature perturbations using a Morlet wavelet of wave number 6 and isolates individual wave packets (i.e., individual gravity waves) in altitude and frequency from the overall wavelet power spectra. The temperature and wind perturbations for each wave packet are then reconstructed using wavelet inversion techniques [*Torrence and Compo*, 1998]. Once these perturbation parameters are determined, the direction of propagation of the gravity wave can be calculated for each wave packet. For the data presented in this paper the number of wave packets per profile ranges from 1 to 6, with wave packets of different vertical wavelength occurring over the same altitude range being distinguishable using the *Zink and Vincent* [2001] technique.

[11] Figure 4 shows an example of a hodograph (using the data in Figure 3) for an individual wave packet; in this example, the resulting hodograph is roughly elliptical in shape. The amplitude of the wave in this example is quite small (~0.6 m/s), the amplitudes seen in the radiosonde data vary from 0.4 m/s to around 2.5 m/s. *Plougonven et al.* [2008] used Vorcore balloons to study a single intense gravity wave event over the Antarctic Peninsula. They simulated the wave given the airflow over the Peninsula to show that the vertical wavelength was ~15 km and that in the lower stratosphere it maximized on the leeward side of the Peninsula. They showed that more typical wave amplitudes in the Peninsula region were ~2 m/s.

[12] This type of plot enables information on the wave's horizontal propagation direction relative to the background wind [*Venkat Raman et al.*, 2009] and vertical energy propagation direction to be determined. In the Southern Hemisphere, owing to the Coriolis effect, an anticlockwise rotation of the gravity-horizontal wave wind vector is associated with a wave having upward energy propagation and downward phase velocity (the opposite is true for the Northern Hemisphere) [*Hirota and Niki*, 1985]. Conversely, clockwise rotation of the gravity wave horizontal wind vector is associated with downward energy propagation and upward phase velocity. The horizontal propagation direction lies along the major axis of the elliptical hodograph.

[13] Two methods to determine the horizontal propagation direction were examined for this work: First the Stokes parameter method [*Vincent et al.*, 1997] combined with cross *S* transform [*Stockwell et al.*, 1996] analysis [*Wang et al.*, 2006a] and second conventional hodograph analysis combined with the *S* transform [*Wang et al.*, 2006b]. The Stokes parameter method uses the perturbation velocities to determine the wave direction, the hodograph method calculates the orientation of the major axis of the hodograph ellipse, along which the wave horizontal propagation direction lies. Both techniques provide a horizontal direction that has a 180° ambiguity. By examining the phase difference between the temperature and the horizontal wind velocity along the direction of propagation, the 180° ambiguity can be removed [*Hamilton*, 1991; *Vincent et al.*, 1997].

[14] These two different techniques were both used in order to verify that the horizontal wave direction agreed, thus giving confidence that the 180° ambiguity was being removed correctly. However, on analysis of one complete year of radiosonde data, it was found that around 15% of the two final horizontal propagation directions differed by around 180°, implying the ambiguity was not being reliably resolved. The wave events where this occurred were found to be those for which the phase difference between the temperature and the horizontal velocity along the direction of propagation was close to 0° or ±180°. This phase difference is expected to be ±90° for a monochromatic wave in the absence of strong shear or dissipation [*Vincent and Alexander*, 2000]. It was found that if the data was filtered such that those phase differences which are 20° either side of 0° or ±180° were excluded the agreement between the two techniques was significantly improved; using this filtering technique all the individual differences in the direc-

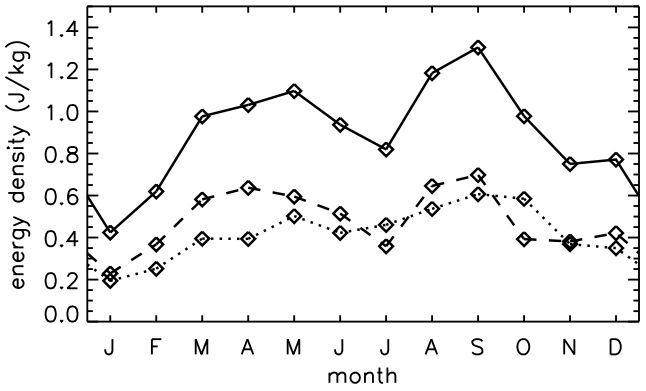

Figure 5. Monthly mean density of kinetic (dashed line) and potential (dotted line) gravity wave energy. Total energy per unit mass (the sum of the kinetic and potential energy density) is shown with a solid line.

tion of propagation between the two derivation methods were within 30° degrees of each other. It is to be expected that there would be a slight difference in the results of the two methods owing to the different techniques used to determine the orientation of the major axis of the ellipse [*Wang et al.*, 2006b]. This filter has therefore been applied to the data used in the propagation direction calculations presented in this paper to ensure that the 180° ambiguity has been removed successfully.

4. Results

4.1. Energy

[15] Figure 5 shows the resulting monthly mean potential and kinetic wave energy density in the lower stratosphere over Rothera. To create the monthly values used in the energy climatologies all the energy densities data for a given month (calculated using equation (1)) were averaged (assuming a lognormal distribution) [*Baumgaertner and McDonald*, 2007] over an altitude range of 15 km to 22 km. The two climatologies show a clear seasonal variation; with the kinetic energy density varying from 0.22 J/kg in the summer to 0.69 J/kg in the spring and the potential energy density varying from 0.19 J/Kg in the summer to 0.60 J/kg in the spring. Both potential and kinetic energy densities peak to a similar value in September, the spring equinox. There is also a lower peak in both energy densities around April/May, with a difference in the kinetic and potential energy density levels (0.63 J/kg compared to 0.50 J/kg, respectively). The spring maximum in gravity wave energy density over Rothera is consistent with other radiosonde lower-stratosphere results from other Antarctic stations [*Yoshiki and Sato*, 2000]. However, the results of *Yoshiki and Sato* [2000] do not show the clear increase in energy after the austral autumn equinox that is seen here at Rothera. A full comparison of our results and those of *Yoshiki and Sato* [2000] will feature in section 6.

[16] *Zangl and Hoinka* [2001] intercalibrated ECMWF Reanalysis data and radiosonde data in an investigation of the polar tropopause. They demonstrated that there is an annual cycle in tropopause pressure in the polar regions and showed that in Antarctica it is at the lowest pressure with coldest temperature in August to September and at the greatest pressure with warmest temperature in February. They determined the tropopause sharpness and demonstrated that no sharp tropopause was present in Antarctica from June to November meaning that it became difficult to define. *Baumgaertner and McDonald* [2007] presented the time-dependent tropopause altitude over 4 years of Antarctic data and showed it to vary from ~9 km in summer to ~13 km in late winter. However, they note that the winter and spring tropopause altitudes will have large uncertainties owing to the difficulty of defining it. If the bend in the temperature profile (the tropopause) is above 15 km then it will bias the PE calculation in this study. Given the uncertainty in defining the tropopause height the relatively large PE in July and October (making the PE/KE ratio larger than unity, which contradicts linear theory) is most likely due to contamination of the temperature variation used in its calculation. *Smith et al.* [2008] show, for example, that the PE/KE ratio can deviate considerably around the tropopause level by factors of 10 in either direction.

4.2. Wave Propagation Direction

4.2.1. Vertical Propagation Direction

[17] The analysis of the wave events in the vertical direction has shown that in the lower stratosphere above Rothera there is a strong seasonal variation in the number of upward and downward propagating gravity waves seen throughout the year. This seasonal variation in the vertical propagation direction of the wave events is illustrated in Figure 6. It shows that in the spring, summer and autumn months (September–May) the upward propagating waves are much more prevalent than downward propagating waves; at this time the upward propagating waves comprise 65% to 91% of the waves observed. In the winter months (June–August) there is a marked increase in the proportion of downward propagating waves, increasing to a maximum of 60% of the total number of waves observed in July. This increase is such that, during the winter months, the downward propagating gravity waves contribute almost as much to the observed stratospheric wave intensity as the upward propagating waves do. In contrast, results from other Ant-

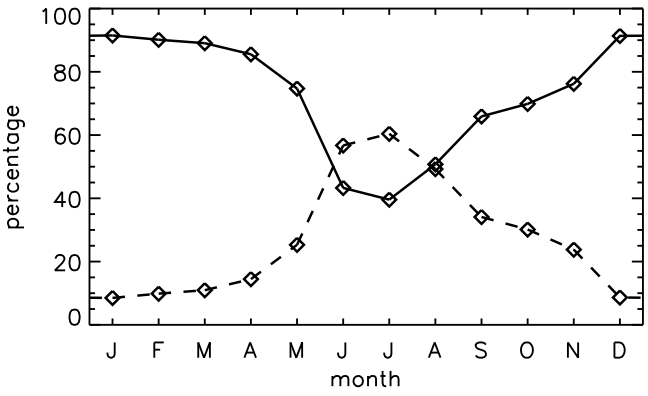

Figure 6. Percentage of upward and downward propagating gravity waves between 15 and 22 km for each month. The upward propagating waves are represented by the solid line; the downward propagating waves are represented by the dashed line.

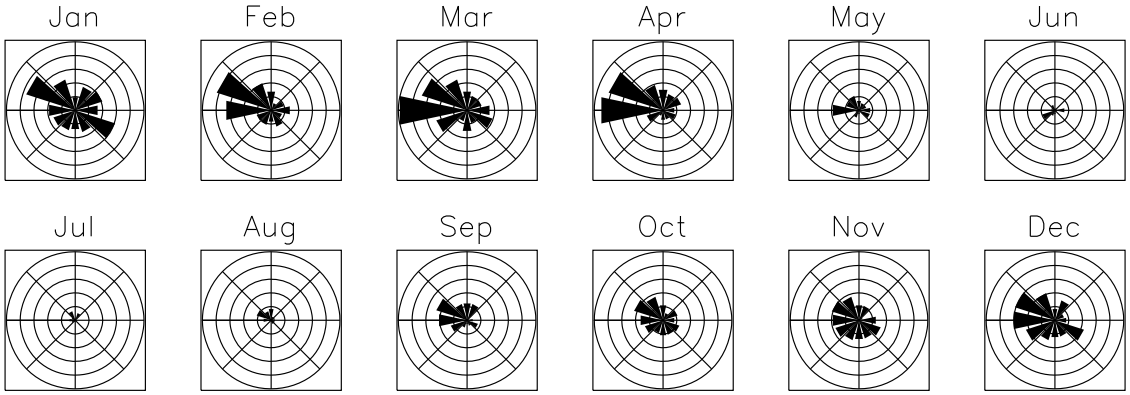

Figure 7. Monthly histograms of horizontal propagation direction of upward propagating gravity waves between 15 and 22 km for 8 years of radiosonde data at Rothera. Each bin represents 30°, and the outer ring on each histogram corresponds to 36 individual wave events. Northward is up, and eastward is to the right.

arctic stations [*Yoshiki and Sato*, 2000] show a dominance of upward propagating waves all year round. *Yoshiki and Sato* [2000] focused primarily on results from Syowa station (69°S, 39°E) and Casey station (66°S, 110°E) and for these stations an increase in downward propagating waves over the late winter (July to August) is seen, although only reaching a maximum of 40% of the total observed waves; this is a lower proportion of the total than what is observed at Rothera.

4.2.2. Horizontal Propagation Direction

[18] Figures 7 and 8 present histograms of the month by month distribution of the horizontal propagation direction for upward and downward propagating gravity waves, respectively. These data are summarized in Figure 9 which shows the average horizontal propagation direction of the wave packets for each month together with the total number of upward and downward propagating waves observed. During the winter months the total number of wave events studied is much smaller than during the summer months. This is a result of the seasonal nature of the eventual burst altitude of the radiosonde balloons which tend to reach lower altitudes in during the winter months than summer, and hence more likely to be excluded from this analysis. However, it can clearly be seen that over the course of the year in the lower stratosphere above Rothera there is a dominance of westward propagating waves for both the upward and downward propagation directions. The upward propagating waves tend toward the northwest during the winter months, although there is considerable variability with typical standard deviations around ±50° about the mean.

[19] Comparing Figures 7 and 8 there is often general agreement, for a particular month, in the distribution pattern of propagation directions between upward and downward propagating waves. This is particularly so in February through October. In the late winter to early spring months of June through September this combines with an approximately equal numbers of waves (see Figure 6) having upward and downward propagation. This is evident in from Figures 7 and 8, taking into account the different scales used for Figures 7 and 8. It can also been seen from Figures 6 and 9. This strongly suggests a dominant source located in the lower stratosphere, possibly the polar vortex, which generates gravity waves both upward and downward simultaneously [*Sato and Yoshiki*, 2008]. In comparison, in February, March and April, the directional spread of upward and downward propagating waves is similar but the number of waves is very dif-

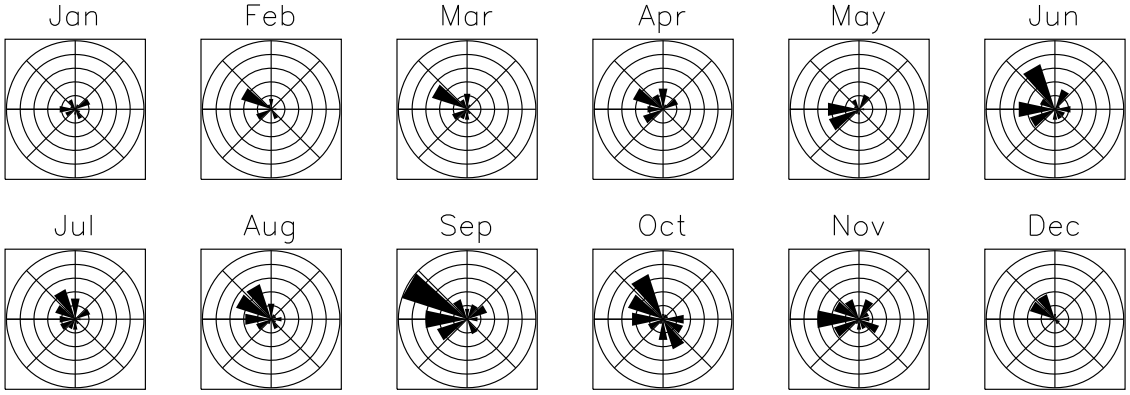

Figure 8. Same as Figure 7 but for downward propagating waves; the outer ring on each histogram corresponds to 13 individual wave events.

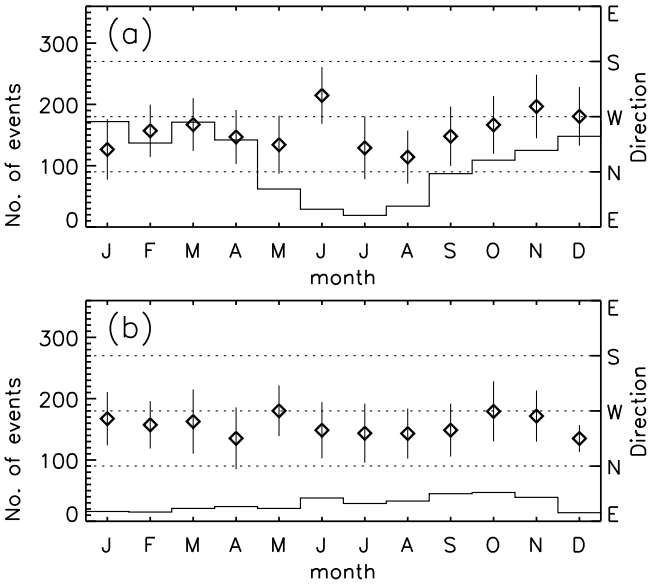

Figure 9. Monthly mean wave horizontal propagation direction (diamonds) for the (a) upward and (b) downward propagating waves observed over Rothera. The standard deviation of the mean is represented by a vertical bar, and the histogram shows the number of wave events included in each month (left-hand scale).

ferent, there being approximately four times as many upward propagating waves as there are downward propagating waves.

5. Discussion

[20] The seasonal variation seen in gravity wave energy density in the lower stratosphere above Rothera is not totally consistent with other Antarctic station radiosonde measurements and measurements taken from satellites. The Challenging Minisatellite Payload/Global Positioning System (CHAMP/GPS) satellite provided radio occultation measurements [*Wickert et al.*, 2004] that allowed the gravity wave potential energy to be determined in regions including the stratosphere above the Antarctic Peninsula. *Baumgaertner and McDonald* [2007] presented CHAMP/GPS results showing the height and time dependence of the potential energy variation integrated over the whole Antarctic continent; the height region analyzed overlaps with the height range analyzed for this paper. Between 15 and 22 km they saw a strong annual variation in potential energy with a single clear peak during August and September. This is consistent with the results derived from the Rothera radiosondes in the same height region for this time of year. However, *Baumgaertner and McDonald* [2007] did not see the smaller increase in potential energy after the autumn equinox that is seen in the Rothera radiosonde data. Both techniques are able to detect a similar part of the gravity wave spectrum so this difference is unlikely to be due to any observational filtering [*Alexander*, 1998]. It is more likely to be attributable to the fact that the measurements of *Baumgaertner and McDonald* [2007] cover the whole continent while those presented here focus solely on the Antarctic Peninsula: if the increase after the autumn equinox is a feature of the Peninsula region alone, then it could become difficult to detect when averaging data across the whole continent. Radiosonde studies of Antarctic continental station data [*Yoshiki and Sato*, 2000] also do not see the postautumn equinox increase in energy density seen at Rothera. Hence, Rothera has been shown to have a different seasonal pattern from the main continent. *Baumgaertner and McDonald* [2007] have also examined the geographical variation in the gravity wavefield over Antarctica. They found increases in potential energy in the lower stratosphere (between 18 and 22 km) occurred over the two main mountainous regions of Antarctica; that is, the Peninsula and the Trans-Antarctic mountains. Correlations between the potential energy in the lower stratosphere and the strength of the NCEP/NCAR 1000 hPa surface zonal wind above the Peninsula region were shown to be statistically significant. *Baumgaertner and McDonald* [2007] suggested that the source of this enhanced gravity wave activity in the lower stratosphere was likely to be orographic wave forcing due to wind flow over topography.

[21] To investigate whether this suggestion can be corroborated in our data, the correlation between the stratospheric gravity wave intensity and surface wind speed has been examined, taking into account the influence on the results of critical-level filtering of mountain waves and nonorographic tropospheric gravity waves. The mean kinetic energy per unit mass between 15 and 22 km for each radiosonde profile was correlated with the mean "surface" wind (the total wind speed measured by the radiosonde between 1 and 2 km), the total wind was used in order to compare directly to the results in the work of *Yoshiki et al.* [2004]. Figure 9 illustrates the monthly correlation values and the corresponding 95% confidence level for each month. This shows that during the winter months (April–August) there is no significant correlation between stratospheric gravity wave intensity and mean surface winds; this is the season when downward propagating waves dominate. It should be noted that Rothera is on the upstream edge of the peninsula and as shown by *Alexander and Teitelbaum* [2007] and *Plougonven et al.* [2008] this will mean that the balloons are not sampling the strongest topographic waves, which tend to extend over the east side of the peninsula. Figure 10 illustrates the monthly correlation values and the corresponding 95% confidence level for each month. This shows that during the winter months (April–August) there is no significant correlation between strato-

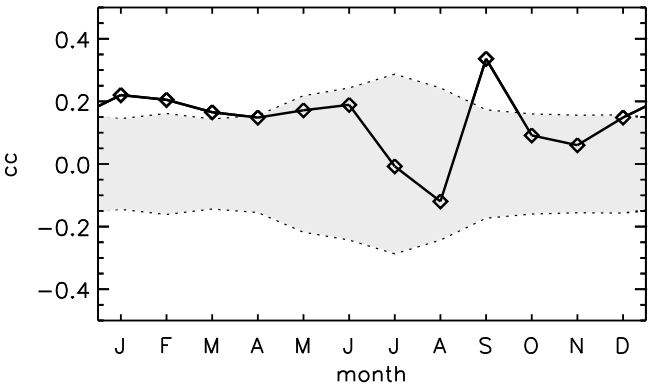

Figure 10. Correlation (solid line) between mean gravity wave kinetic energy density between 15 and 22 km and the "surface" wind (measured between 1 and 2 km). The shaded region represents correlations below the 95% confidence level for each month.

spheric gravity wave intensity and mean surface winds; this agrees well with the seasonal variation of vertical propagation where, for this time frame, downward propagating waves dominate. There is a region of significant correlation at the spring equinox (September) and from January to March. This implies that for these times of year, the gravity wave intensity seen in the lower stratosphere by radiosondes over Rothera is influenced significantly by orographically generated gravity waves. The low values of correlation (although significant) could be because mountain waves can be of a higher frequency (relative to the background winds) to that which the radiosonde is sensitive to. A similar study has been carried out with radiosonde data taken from Syowa station [*Yoshiki et al.*, 2004], where there is a lack of any large-scale orographic features, and they found no significant correlation between the surface winds and the gravity wave intensity in the lower stratosphere.

[22] The intensity of both mountain waves and nonorographic gravity waves that reach the stratosphere from their source regions in the troposphere can be affected by critical-level filtering by the background wind. This has been demonstrated over Rothera, using 471 h of lidar data across 3 years, by *Yamashita et al.* [2009], who used wind-blocking diagrams [*Taylor et al.*, 1993] to determine the probability of the waves reaching a certain altitude. They found that for mountain waves there was ~50% probability of them reaching the stratosphere during the winter months and equinoxes while the probability fell to close to zero during the summer. There was also a slightly greater probability of the mountain waves reaching the stratosphere during the spring equinox than during the autumn equinox. This marked seasonal difference was not present for the nonorographic gravity waves. Over the altitude range from 15 km to 22 km, there was a slightly lower probability that nonorographic waves reached the stratosphere during winter and spring (60–70%) than during summer and autumn (70–80%).

[23] These findings lead to the conclusion that the increases in gravity wave intensity seen around the equinoxes in the Rothera radiosonde data are due to the competing effects of two different sources: mountain waves and the polar vortex. The seasonal variation seen in the intensity is due in part to the variation in critical-level filtering of the gravity waves from the troposphere. The largest peak in gravity wave intensity seen in the spring relates to the slightly higher probability of mountain waves reaching the stratosphere during the spring equinox combined with the increased downward propagating wave activity in spring (compared to the summer levels of activity). The enhanced gravity wave energy density seen in winter compared to summer appears to be related to the increased downward propagating waves seen in these data during winter. The seasonal variation in wave energy whereby there is a greater energy density in winter than in summer is also likely to be strongly influenced by the seasonal variation in the first-order basic atmospheric characteristics which affect the static stability and hence the propagation and saturation of gravity waves. *Eckermann* [1995] showed that (in the Northern Hemisphere) at high latitudes if height variations in the background wind and possible seasonal variation in wave source strengths are ignored, then the modeled gravity wave activity measured as horizontal velocity variance at the top of the stratosphere is a factor of two greater in winter than in summer. He corroborated those calculations with observational evidence from rocket-based measurements. This first-order annual pattern is similar to that shown in Figure 5 for Rothera ignoring the equinoctal peaks, albeit in the lower stratosphere.

[24] The exact source of the downward propagating gravity waves during the winter and spring months is not clear from the data used in this study. However, previous work [*Sato and Yoshiki*, 2008; *Yamashita et al.*, 2009; *Yoshiki et al.*, 2004], has shown that during the Austral winter the Antarctica polar stratospheric vortex is at its strongest and when it starts to break up in the springtime, an increase in wave energy can occur owing to the wave generation at its edge. At the same time it has been shown that there is an increase in the number of downward propagating gravity waves generated, compared to upward propagating gravity waves, at the edge of the vortex [*Sato and Yoshiki*, 2008].

[25] The horizontal propagation direction of the upward gravity waves in the lower stratosphere shows a strong westward tendency throughout the year, implying that there is a net filtering of eastward propagating waves by the tropospheric westerly winds above Rothera [*Hibbins et al.*, 2005]. The vertical flux of horizontal momentum carried by gravity waves into the mesosphere has been measured above Rothera using combined airglow imager and MF radar data [*Espy et al.*, 2006]. However, owing to the operational restraints of the airglow imager (it requires dark conditions to operate) the momentum fluxes can only be determined between March and September at this latitude. *Espy et al.* [2006] showed that the zonal momentum flux was largely westward and northward around the winter solstice and that there was a decrease in the westward prevalence of the zonal momentum flux toward the equinoxes. Although the two instruments (the airglow imager and the radiosonde) will be looking at slightly different parts of the gravity wave spectrum [*Alexander*, 1998], the seasonal variation of the mesospheric direction of momentum flux shown in the work of *Espy et al.* [2006] agree well with the seasonal variation in the gravity wave horizontal propagation direction from the lower stratosphere shown in this paper. *Espy et al.* [2006] hypothesized that the large values of zonal momentum flux, and its seasonal variation, seen in the mesosphere above Rothera were related to a large gravity wave source being present (i.e., Rothera's location on the mountainous Peninsula) and to critical-level filtering of the gravity wavefield by the stratospheric winds. The results in this paper show that such a gravity wave source is indeed present in the stratosphere. These results emphasize the need to fully quantify the variations of gravity wave activity at all frequencies throughout the atmosphere in order to understand the vertical coupling effects of gravity waves and their influence on polar atmospheric circulation.

6. Conclusions

[26] Eight years of radiosonde data from Rothera (67°S, 68°W), Antarctica have been used to examine gravity wave activity in the lower stratosphere. The potential and kinetic energy densities of gravity waves undergo a strong seasonal variation with a large increase in intensity near the spring equinox and a smaller increase after the autumn equinox. This seasonal variation has been attributed to a combination of factors: the seasonal variation of critical-level wind filtering (the wind variations from the radiosonde data can be seen in the work of *Hibbins et al.* [2005, Figure 2]) of mountain

waves and nonorographic gravity waves from the troposphere plus the seasonal variation in the numbers of upward and downward propagating waves, possibly related to the polar stratospheric vortex. The underlying annual variation is likely to be influenced is likely to be influenced by the summer to winter contrast in basic atmospheric characteristics which affect the wave growth and saturation through variations in static stability.

[27] Analysis of the vertical propagation direction of the wave events shows that there are seasonal variations in the percentage of gravity waves propagating both upward and downward. During the winter months of June and July the majority of wave events studied are found to be downward propagating, but throughout the rest of the year upward propagating waves make up the majority of the waves observed.

[28] The results of this paper have determined that the seasonal variation in lower stratospheric, low-frequency gravity wave intensity (i.e., waves observable by radiosondes) above Rothera, situated on the Antarctic Peninsula, differs from that seen on the main Antarctic Continent. At Rothera there are clear increases in the intensity around both equinoxes, especially the spring equinox, which are not seen in studies from locations on the main Antarctic Continent. The Peninsula region is already known to have a "hotspot" of gravity wave activity [*Ern et al.*, 2004] that is not seen over the main continent although the exact nature of the sources of this gravity wave activity are not clear, with studies suggesting different competing sources contributing to the main orographic source (e.g., stratospheric jets or tropospheric features) [*Yamashita et al.*, 2009; *Yoshiki and Sato*, 2000]. This paper has investigated the likely sources of low-frequency inertia-gravity waves in the lower stratosphere and has shown that different sources dominate over the course of a year. The seasonal variation of downward propagating waves and the critical-level filtering of upward propagating waves (both mountain and nonorographic waves) are equally important in explaining the gravity wave activity seen in the lower stratosphere above the Peninsula.

[29] The extensive nature of the radiosonde data set from Rothera will enable more detailed investigations of the climatological variations and interyear variations of both tropospheric and stratospheric gravity wave parameters in the important wave generation region of the Antarctic Peninsula. Such studies will be vital to further understanding of the gravity wave sources and their variability over the Peninsula and the effect of vertical coupling between the lower atmosphere and the mesosphere and thermosphere.

[30] **Acknowledgment.** We acknowledge the hard work of the Rothera field staff, who have helped to maintain the radiosonde program throughout the past 8 years.

References

Alexander, M. J. (1998), Interpretations of observed climatological patterns in stratospheric gravity wave variance, *J. Geophys. Res.*, *103*, 8627–8640, doi:10.1029/97JD03325.

Alexander, M. J., and H. Teitelbaum (2007), Observation and analysis of a large amplitude mountain wave event over the Antarctic Peninsula, *J. Geophys. Res.*, *112*, D21103, doi:10.1029/2006JD008368.

Alexander, M. J., et al. (2008), High-resolution satellite observations of mountain waves, *Bull. Am. Meteorol. Soc.*, *89*, 151–152.

Alexander, M. J., et al. (2010), Recent developments in gravity-wave effects in climate models and the global distribution of gravity-wave momentum flux from observations and models, *Q. J. R. Meteorol. Soc.*, *136*, 1103–1124.

Allen, S. J., and R. A. Vincent (1995), Gravity wave activity in the lower atmosphere: Seasonal and latitudinal variations, *J. Geophys. Res.*, *100*, 1327–1350, doi:10.1029/94JD02688.

Baumgaertner, A. J. G., and A. J. McDonald (2007), A gravity wave climatology for Antarctica compiled from Challenging Minisatellite Payload/Global Positioning System (CHAMP/GPS) radio occultations, *J. Geophys. Res.*, *112*, D05103, doi:10.1029/2006JD007504.

Cariolle, D., S. Muller, F. Cayla, and M. P. McCormick (1989), Mountain waves, polar stratospheric clouds and the ozone depletion over Antarctica, *J. Geophys. Res.*, *94*, 11,233–11,240, doi:10.1029/JD094iD09p11233.

Eckermann, S. D. (1995), On the observed morphology of gravity-wave and equatorial-wave variance in the stratosphere, *J. Atmos. Terr. Phys.*, *57*, 105–134, doi:10.1016/0021-9169(93)E0027-7.

Ern, M., P. Preusse, M. J. Alexander, and C. D. Warner (2004), Absolute values of gravity wave momentum flux derived from satellite data, *J. Geophys. Res.*, *109*, D20103, doi:10.1029/2004JD004752.

Espy, P. J., et al. (2006), Regional variations of mesospheric gravity-wave momentum flux over Antarctica, *Ann. Geophys.*, *24*, 81–88, doi:10.5194/angeo-24-81-2006.

Fritts, D. C., and M. J. Alexander (2003), Gravity wave dynamics and effects in the middle atmosphere, *Rev. Geophys.*, *41*(1), 1003, doi:10.1029/2001RG000106.

Guharay, A., M. Venkat Ratnam, D. Nath, and U. C. Dumka (2010), Investigation of saturated gravity waves in the tropical lower atmosphere using radiosonde observations, *Radio Sci.*, *45*, RS6008, doi:10.1029/2010RS004372.

Hamilton, K. (1991), Climatological statistics of stratospheric inertia-gravity waves deduced from historical rocketsonde wind and temperature data, *J. Geophys. Res.*, *96*, 20,831–20,839.

Hertzog, A., et al. (2008), Estimation of gravity wave momentum flux and phase speeds from quasi-Lagrangian stratospheric balloon flights. part II: Results from the Vorcore campaign in Antarctica, *J. Atmos. Sci.*, *65*, 3056–3070, doi:10.1175/2008JAS2710.1.

Hibbins, R. E., et al. (2005), Seasonal variations in the horizontal wind structure from 0–100 km above Rothera station, Antarctica, *Atmos. Chem. Phys. Disc.*, *5*, 4291–4310, doi:10.5194/acpd-5-4291-2005.

Hibbins, R. E., et al. (2007), A climatology of tides and gravity wave variance in the MLT above Rothera, Antarctica, obtained by MF radar, *J. Atmos. Sol. Terr. Phys.*, *69*, 578–588, doi:10.1016/j.jastp.2006.10.009.

Hirota, I., and T. Niki (1985), A statistical study of inertia-gravity waves in the middle atmosphere, *J. Meteorol. Soc. Jpn.*, *63*, 1055–1066.

Hoepfner, M., et al. (2006), MIPAS detects Antarctic stratospheric belt of NAT PSCs caused by mountain waves, *Atmos. Chem. Phys.*, *6*, 1221–1230, doi:10.5194/acp-6-1221-2006.

Ki, M.-O., and H.-Y. Chun (2010), Characteristics and sources of inertia-gravity waves revealed in the KEOP-2007 radiosonde data, *J. Atmos. Sci.*, *46*, 261–277.

Kim, Y.-J., et al. (2003), An overview of the past, present and future of gravity wave drag parameterisation for numerical climate and weather prediction models, *Atmos. Ocean*, *41*, 65–98, doi:10.3137/ao.410105.

McDonald, A. J., et al. (2009), Can gravity waves significantly impact PSC occurrence in the Antarctic?, *Atmos. Chem. Phys.*, *9*, 8825–8840, doi:10.5194/acp-9-8825-2009.

McDonald, A. J., B. Tan, and X. Chu (2010), Role of gravity waves in the spatial and temporal variability of stratospheric temperature measured by COSMIC/FORMOSAT-3 and Rayleigh lidar observations, *J. Geophys. Res.*, *115*, D19128, doi:10.1029/2009JD013658.

McLandress, C., and J. F. Scinocca (2005), The GCM response to current parameterizations of nonorographic gravity wave drag, *J. Atmos. Sci.*, *62*, 2394–2413, doi:10.1175/JAS3483.1.

Nastrom, G. D., and D. C. Fritts (1992), Sources of mesoscale variability of gravity waves. Part I: Topographic excitation, *J. Atmos. Sci.*, *49*, 101–110, doi:10.1175/1520-0469(1992)049<0101:SOMVOG>2.0.CO;2.

Noel, V., A. Hertzog, H. Chepfer, and D. M. Winker (2008), Polar stratospheric clouds over Antarctica from the CALIPSO spaceborne lidar, *J. Geophys. Res.*, *113*, D02205, doi:10.1029/2007JD008616.

Plougonven, R. A. Hertzog, and H. Teitelbaum (2008), Observations and simulations of a large-amplitude mountain wave breaking over the Antarctic Peninsula, *J. Geophys. Res.*, *113*, D16113, doi:10.1029/2007JD009739.

Preusse, P., A. Dörnbrack, S. D. Eckermann, M. Riese, B. Schaeler, J. T. Bacmeister, D. Broutman, and K. U. Grossmann (2002), Space-based measurements of stratospheric mountain waves by CRISTA: 1. Sensitivity, analysis method, and a case study, *J. Geophys. Res.*, *107*(D23), 8178, doi:10.1029/2001JD000699.

Sato, K., and M. Yoshiki (2008), Gravity wave generation around the polar vortex in the stratosphere revealed by 3-hourly radiosonde obser-

vations at Syowa station, *J. Atmos. Sci.*, *65*, 3719–3735, doi:10.1175/2008JAS2539.1.

Smith, R., et al. (2008), Mountain waves enerting the stratosphere, *J. Atmos. Sci.*, *65*, 2543–2562, doi:10.1175/2007JAS2598.1.

Steinbrecht, W., et al. (2008), Pressure and temperature differences between Vaisala RS80 and RS92 radiosonde systems, *J. Atmos. Oceanic Technol.*, *25*, 909–927, doi:10.1175/2007JTECHA999.1.

Stockwell, R. G., et al. (1996), Localization of the complex spectrum: The S transform, *IEEE Trans. Signal Process.*, *44*, 998–1001, doi:10.1109/78.492555.

Taylor, M. J., E. H. Ryan, T. F. Tuan, and R. Edwards (1993), Evidence of preferential directions for gravity wave propagation due to wind filtering in the middle atmosphere, *J. Geophys. Res.*, *98*, 6047–6057, doi:10.1029/92JA02604.

Torrence, C., and G. P. Compo (1998), A practical guide to wavelet analysis, *Bull. Am. Meteorol. Soc.*, *79*, 61–78, doi:10.1175/1520-0477(1998)079<0061:APGTWA>2.0.CO;2.

Venkat Raman, M., et al. (2009), Characteristics of gravity waves observed with intensive radiosonde campaign during November–December 2005 over western Sumatera, *Earth Planets Space*, *61*, 983–993.

Vincent, R. A., and M. J. Alexander (2000), Gravity waves in the tropical lower stratosphere: An observational study of seasonal and interannual variability, *J. Geophys. Res.*, *105*, 17,971–17,982.

Vincent, R. A., et al. (1997), Gravity-wave parameters in the lower stratosphere, in *Gravity Wave Processes: Their Parameterization in Global Climate Models*, edited by K. Hamilton, pp. 7–25, Springer, New York.

Wang, L., et al. (2006a), Small-scale gravity waves in ER-2 MMS/MTP wind and temperature measurements during CRYSTAL-FACE, *Atmos. Chem. Phys.*, *6*, 1091–1104, doi:10.5194/acp-6-1091-2006.

Wang, L., et al. (2006b), Gravity waves in the middle atmosphere during the MaCWAVE winter campaign: Evidence of mountain wave critical level encounters, *Ann. Geophys.*, *24*, 1209–1226, doi:10.5194/angeo-24-1209-2006.

Whiteway, J. A., T. J. Duck, D. P. Donovan, J. C. Bird, S. R. Pal, and A. I. Carswell (1997), Measurements of gravity wave activity within and around the Arctic stratospheric vortex, *Geophys. Res. Lett.*, *24*, 1387–1390, doi:10.1029/97GL01322.

Wickert, J., et al. (2004), The radio occultation experiment aboard CHAMP: Operational data analysis and validation of vertical atmospheric profiles, *J. Meteorol. Soc. Jpn.*, *82*, 381–395, doi:10.2151/jmsj.2004.381.

Wu, D. L., and J. H. Jiang (2002), MLS observations of atmospheric gravity waves over Antarctica, *J. Geophys. Res.*, *107*(D24), 4773, doi:10.1029/2002JD002390.

Yamashita, C., X. Chu, H.-L. Liu, P. J. Espy, G. J. Nott, and W. Huang (2009) Stratospheric gravity wave characteristics and seasonal variations observed by lidar at the South Pole and Rothera, Antarctica, *J. Geophys. Res.*, *114*, D12101, doi:10.1029/2008JD011472.

Yan, X., N. Arnold, and J. Remedios (2010), Global observations of gravity waves from High Resolution Dynamics Limb Sounder temperature measurements: A year-long record of temperature amplitude and vertical wavelength, *J. Geophys. Res.*, *115*, D10113, doi:10.1029/2008JD011511.

Yoshiki, M., and K. Sato (2000), A statistical study of gravity waves in the polar regions based on operational radiosonde data, *J. Geophys. Res.*, *105*, 17,995–18,011.

Yoshiki, M., N. Kizu, and K. Sato (2004), Energy enhancements of gravity waves in the Antarctic lower stratosphere associated with variations in the polar vortex and tropospheric disturbances, *J. Geophys. Res.*, *109*, D23104, doi:10.1029/2004JD004870.

Zangl, G., and K. P. Hoinka (2001), The tropopause in the polar regions, *J. Clim.*, *14*, 3117–3139, doi:10.1175/1520-0442(2001)014<3117:TTITPR>2.0.CO;2.

Zhang, S. D., et al. (2010), Latitudinal and seasonal variations of lower atmospheric inertial gravity wave energy revealed by U.S. radiosonde data, *Ann. Geophys.*, *28*, 1065–1074, doi:10.5194/angeo-28-1065-2010.

Zink, F., and R. Vincent (2001), Wavelet analysis of stratospheric gravity wave packets over Macquarie Island: 1. Wave parameters, *J. Geophys. Res.*, *106*, 10,275–10,288.

S. R. Colwell, M. J. Jarvis, and T. Moffat-Griffin, British Antarctic Survey, High Cross, Madingley Rd., Cambridge CB3 0ET, UK. (tmof@bas.ac.uk)

R. E. Hibbins, Department of Physics, Norwegian University of Science and Technology, N-7491 Trondheim, Norway.